

# X-ray Dichroism in Noncentrosymmetric crystals

Paolo Carra, Andres Jerez, and Ivan Marri<sup>†</sup>

European Synchrotron Radiation Facility, B.P. 220, F-38043 Grenoble Cedex, France

(Dated: March 22, 2024)

In this paper the authors analyse near-edge absorption of x-rays in noncentrosymmetric crystals. The work is motivated by recent observations of x-ray dichroic effects which stem from parity-nonconserving electron interactions. We provide a theoretical description of these experiments and show that they are sensitive to microscopic polar and magnetoelectric properties of the sample. Our derivation extends previous theoretical work on centrosymmetric systems and identifies new directions in the microscopic analysis of crystalline materials using x-ray absorption spectroscopy.

PACS numbers: PACS numbers: 78.70.Dm, 33.55.Ad

## I. INTRODUCTION

### A. Pure electric transitions

Near-edge x-ray dichroism with synchrotron radiation is a powerful probe of electronic states in crystals. As is known, its effectiveness stems from two prominent features of inner-shell excitations

site selectivity, resulting from the tuning of the x-ray energy at a given inner-shell threshold;

electron angular momentum resolution, as enforced by the selection rules of pure electric multipole (E1, E=2, ...) transitions, which raise an inner-shell electron to empty valence orbitals.

Linear or circular polarisations are employed in experiments, leading to linear or circular x-ray dichroism, respectively. The former implies a difference between radiations with linear polarisations parallel or perpendicular to a local symmetry axis and is sensitive to charge anisotropies. The latter measures the difference in absorption between right and left circularly polarised radiations and reflects magnetic properties of crystals.

Following the pioneering work of Templeton and Templeton [1] and Schutz and coworkers [2], a number of authors have recorded x-ray dichroic signals in a variety of samples, ranging across the periodic table from 3d transition metals to actinides.

In parallel with this experimental activity, theory has aimed at identifying the microscopic origin of the observed spectra. Working within an atomic model [3, 4, 5] (a good approximation, as it was later demonstrated [6]) a set of sum rules was obtained, which relate integrated dichroic intensities to the ground-state expectation value of effective one-electron operators (irreducible tensors) [7]. Two classes of operators are obtained, which are identified by their transformation properties under space

inversion ( $x \rightarrow -x$ , I-transformation) and time reversal ( $t \rightarrow -t$ , R-transformation). They correspond to charge (I-even, R-even) and magnetic (I-even, R-odd) order parameters of crystals. X-ray dichroism is thus sensitive to long-range crystalline orderings; and these are distinguished by photon polarisation and by the nature (E1 or E2) of the inner-shell excitation. Undoubtedly, the most important result of this theoretical analysis has been to show that, in a ferromagnet (or ferrimagnet), x-ray circular dichroism provides a direct and independent determination of orbital and spin contributions to the magnetic moment [3, 4].

It is important to observe that pure electric multipole transitions cannot probe electronic properties which stem from the breaking of space inversion: all order parameters revealed by pure E1 and E2 transitions are even under the transformation I.

### B. Interference

In the x-ray region, other classes of dichroic phenomena have recently been investigated by Goulon et al. who reported the observation of three effects:

X-ray natural circular dichroism (XNCD), probed in  $\text{Na}_3\text{Nd}(\text{digly})_3 \cdot 2\text{NaBF}_4 \cdot 6\text{H}_2\text{O}$  [8] and in  $-\text{LiTiO}_3$  [9]. (The effect was observed near the Nd  $L_3$  edge and near the iodine L edges.)

X-ray nonreciprocal linear dichroism (XNLD), detected near the vanadium K edge in the low-temperature insulating phase of a Cr-doped  $\text{V}_2\text{O}_3$  crystal [10].

X-ray magnetochiral dichroism (XMCD), observed at the chromium K edge [11] in crystalline  $\text{Cr}_2\text{O}_3$ .

Here, inner-shell excitations are ascribed to the E1-E2 interference; detecting a nonvanishing signal thus requires an ordered structure and the breaking of space inversion.

In our view, the work of Goulon and his collaborators is of particular importance as it identifies new directions in the microscopic analysis of materials using x-ray absorption spectroscopy. In fact, symmetry considerations

<sup>†</sup>Electronic address: carra@esrf.fr

<sup>†</sup>Also at INFN and Dipartimento di Fisica dell'Università degli Studi di Modena e Reggio Emilia, 41100 Modena, Italy.



TABLE I: Order parameters and x-ray dichroic effects.

Order Parameter	Space Inversion	Time Reversal	X-ray Dichroism	X-ray Transition
Charge	even	even	Linear	Pure E1 or E2
Magnetic	even	odd	Magnetic Circular	Pure E1 or E2
Electric	odd	even	Natural Circular	Interference E1-E2
Magnetoelectric	odd	odd	Nonreciprocal	Interference E1-E2

Four operators  $O^{(i)}$  contribute to the E1-E2 absorption spectrum for arbitrary polarisation. They can all be written out in terms of three dimensionless order parameters: the familiar orbital angular momentum  $L$ , an

electric dipole  $n = r \cdot r$ , and  $\hat{n} = (n \cdot L - L \cdot n)/2$ , a ME vector.

By applying suitable recoupling transformations to Eq. (1), we obtain

$$O^{(1)} = \hat{n}; \quad O^{(2+)} = [L; j^{(2)}]; \quad O^{(2)} = [L; n]^{(2)} \quad \text{and} \quad O^{(3)} = [L; L]^{(2)}; j^{(3)}; \quad (4)$$

where the couplings are defined via Clebsch-Gordan coefficients

$$[U^{(p)}; V^{(i)}]_q^{(k)} = \sum_{p,q} C_p^{kq} U^{(p)} V^{(i)};$$

Equations (4) identify one-electron properties revealed by E1-E2 absorption in the x-ray domain. The corresponding geometrical factors are given in Table II. As  $T^{(1+)}(\hat{k}) = T^{(3+)}(\hat{k}) = 0$ , the polar moments  $O^{(1+)} = n$  and  $O^{(3+)} = [L; L]^{(2)}; n]^{(3)}$  do not contribute to expression (2).]

Our derivation is based on a localised model, which considers a single ion with a partially filled valence shell; all other shells filled. Inclusion of spin-orbit interactions and/or crystal fields results in a deformation of the electronic cloud. Its multipolar expansion will contain spin and orbital moments characteristic of the symmetry of the deformation and described by one-particle irreducible tensors. Valence states are hybridised in general, with the orbital part given as a superposition of two angular momenta:  $l$  and  $l^0 = l - 1$ , corresponding to  $sp$  or  $pd$  hybridisation in the actual case. (In our formalism, valence electrons are labelled using uncoupled orbital and spin quantum numbers.)

As shown in previous work [3, 4, 5], integrated dichroic spectra which stem from pure E1 or E2 transitions provide a measure of the ground-state expectation value of I-even irreducible tensors. Only the diagonal part (in the sense of  $|j, l^0\rangle$ ) contributes to the ground-state matrix elements in this case. Angular momentum and parity are good quantum numbers; the known sum rules for linear and circular dichroism are recovered [15].

Integrated E1-E2 dichroic spectra are related to the ground-state expectation value of I-odd irreducible ten-

sors. Only the off-diagonal part contributes to the ground-state matrix elements, in this case. Orbital angular momentum is not a good quantum number and

TABLE II: Polarisation responses of the E1-E2 interference.

$T^{(1)}(\hat{k})_2 = \frac{1}{2} \frac{q}{5} \hat{k}$
$T^{(2+)}(\hat{k})_2 = \frac{p-3}{2} [[L; j^{(1)}]; \hat{k}]^{(2)}$
$T^{(2)}(\hat{k})_2 = \frac{h}{2} [L; j^{(2)}; \hat{k}]^{i_{(2)}}$
$T^{(3)}(\hat{k})_2 = \frac{h}{2} [L; j^{(2)}; \hat{k}]^{i_{(3)}}$

electron states do not have definite parity. Hybridisation effects are now observable and described by the operators  $O^{(i)}$ .

Relations between XNCD, XNLD, XMCD and the order parameters given by Eqs. (4) will be provided below.

## B. Interpretation of experiments

### 1. XNCD

In this case, a recoupling of Eq. (1) leads to the following integral relation

$$\sum_{j+j_+}^Z \frac{\chi_{j+j_+}^{(+)}(\mathbf{l})}{(\sim \mathbf{l})^2} d(\sim \mathbf{l}) = \frac{16}{3\sim c} (2l_c + 1) \sum_{\substack{l=l_c \\ l^0=1}}^X \sum_{\substack{l=1 \\ l^0=1}}^X R_{l_c 1}^{(1)} R_{l_c l^0}^{(2)} a_{l^0}^{(2;+)}(l_c; \mathbf{l}) \left( \frac{r}{2} T_q^{(2;+)}(\mathbf{l}; \mathbf{l}^0; \hat{k}) \text{hgj} \mathbb{L}; \mathbf{l}_q^{(2)}(l; l^0) \text{gji}; \right) \quad (5)$$

which reveals the microscopic origin of XNCD spectra. Here,  $\mathbf{l} = (i=2)(\mathbf{l}_1 \mathbf{l}_2)$  denote circular polarisa-

tion states; the index  $q$  runs over valence electrons [16]. Furthermore,

$$a_{l^0}^{(2;+)}(l_c; \mathbf{l}) = \frac{2(2l+1)(2l^0+1)[6+3l_c(l_c+1)-2l(l+1)-l^0(l^0+1)]}{(l+l^0+1)(l_c-3l^0+2l)(l_c+3l^0-2l+1)(l_c+1)^2(l_c+1+2)^2} : \quad (6)$$

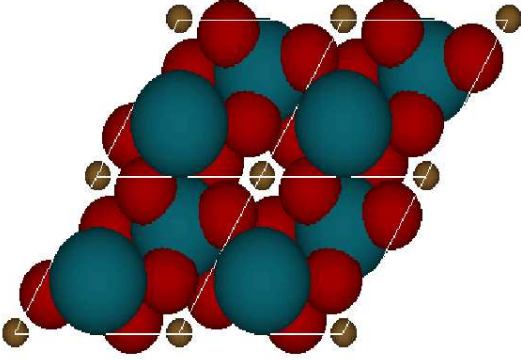


FIG. 1: Crystal structure of  $-\text{LiIO}_3$ , with  $\text{Li}$  = Li,  $\text{O}$  = O, and  $\text{I}$  = I.

The XNCD experiment of Goulon et al. on  $-\text{LiIO}_3$  [9], whose crystal structure (space group  $P6_3$ ) is depicted in Fig. 1, is readily interpreted with the help of Eq. (5).

We focus on charge properties stemming from  $sp$  hybridisation. (The 4d shell of iodine is filled and the crys-

tal displays no magnetism.) At the iodine sites the symmetry is  $C_3$ . Notice that  $O^{(2;+)} = [\mathbb{L}; \mathbf{j}]^{(2)}$ , known as pseudodeviator or gyration tensor, is totally symmetric in this point group i.e., it is invariant under all  $C_3$  transformations. It yields therefore a nonvanishing ground-state expectation value at each iodine site. The three-fold axes of all the iodate groups are parallel in the unit cell of  $-\text{LiIO}_3$  ( $P6_3$  is noncentrosymmetric). As a consequence, all the microscopic pseudodeviators add up upon absorption of circularly polarised x rays. This contribution to the E1-E2 absorption profile is selected by circular dichroism (see Table II) yielding the observed XNCD spectrum. The effect can thus be viewed as the I-odd analog of ferroquadrupolar ordering, which is probed by pure E1 x-ray linear dichroism [5].

## 2. XNLD

In the case of XNLD, the integral relation reads

$$\sum_{j+j_+}^Z \frac{\chi_{j+j_+}^{(k)}(\mathbf{l}) \chi_{j+j_+}^{(?) }(\mathbf{l})}{(\sim \mathbf{l})^2} d(\sim \mathbf{l}) = \frac{8}{\sim c} (2l_c + 1) \sum_{\substack{l=l_c \\ l^0=1}}^X \sum_{\substack{l=1 \\ l^0=1}}^X R_{l_c 1}^{(1)} R_{l_c l^0}^{(2)} \sum_q^X \left( \frac{r}{2} a_{l^0}^{(2;)}(l_c; \mathbf{l}) i T_q^{(2;)}(\mathbf{l}; \mathbf{l}^0; \hat{k}) T_q^{(2;)}(\mathbf{l}; \mathbf{l}^0; \hat{k}) \right. \\ \left. \text{hgj} \mathbb{L}; \mathbf{n} \mathbf{l}_q^{(2)}(l; l^0) \text{gji} - 2a_{l^0}^{(3;)}(l_c; \mathbf{l}) T_q^{(3;)}(\mathbf{l}; \mathbf{l}^0; \hat{k}) T_q^{(3;)}(\mathbf{l}; \mathbf{l}^0; \hat{k}) \text{hgj} \mathbb{L}; \mathbf{l} \mathbf{l}^0 \right) \mathbf{l}_q^{(3)}(l; l^0) \text{gji}; \quad (7)$$

where  $k$  and  $?$  denote two orthogonal linear-polarisation states. The expansion coefficients are given by

$$a_{l^0}^{(3;)}(l_c; \mathbf{l}) = \frac{a_{l^0}^{(2;+)}(l_c; \mathbf{l})}{6+3l_c(l_c+1)-2l(l+1)-l^0(l^0+1)} \quad (8)$$

and

$$a_{l^0}^{(2;)}(l_c; \mathbf{l}) = \frac{(l+l^0+1)(l^0-1)}{2} a_{l^0}^{(2;+)}(l_c; \mathbf{l}); \quad (9)$$

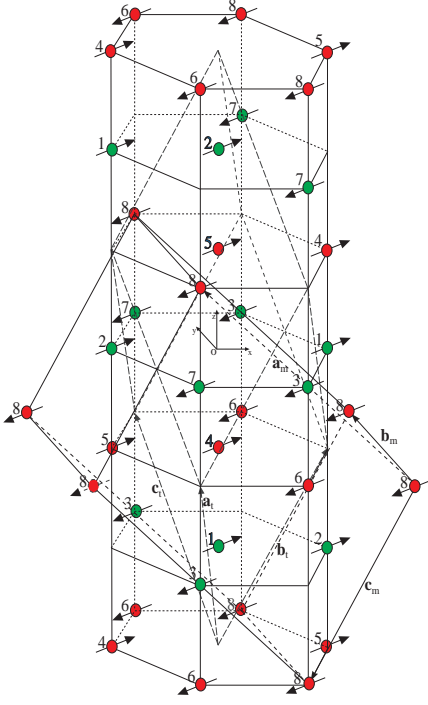


FIG. 2: Corundum and monoclinic structures of  $V_2O_3$ . ( and denote different orientations of the oxygen octahedra.) The AFM structure is also displayed.

with  $a_{j0}^{(2;+)}(l_e; l)$  defined by Eq. (6).

Equation (7) reveals the microscopic ME nature of XNLD. (Notice the peculiarity of this form of linear dichroism: it changes sign upon reversal of an external applied magnetic field [17]. The result implies that Goulon and his co-workers have probed ME properties of  $(V_{1-x}Cr_x)_2O_3$ .

$V_2O_3$  is characterised by a strongly destructive first-order transition from a paramagnetic metallic phase (corundum structure) to an antiferromagnetic (AFM) insulating phase (monoclinic) at  $T_N = 150$  K. The unit cells of pure  $V_2O_3$  are depicted in Fig. 2.

Substitution of  $Cr^{3+}$  in the  $V_2O_3$  lattice results in a Mott metal-to-insulator transition. At room temperature, charge properties of the compound can be deduced from structural studies, which have been reported by Demier and Marzio [18, 19]. These authors ascribe the Cr-induced metal-to-insulator transition to an increase in the nearest neighbour vanadium-vanadium distances, which is accompanied by an ‘umbrella-like’ distortion of the oxygen octahedra. Crystal-structure refinements indicate that at each vanadium site the point group is  $C_{3v}$  [19]. Formation of an electric-dipole moment is thus permitted by symmetry. Crystallography also suggests that nearest-neighbour pairs of vanadium atoms are antiferroelectrically ordered along the hexagonal c axis (the symmetry of a pair is  $D_{3h}$  [19]), as shown in Fig. 3. We can thus argue that, at about 300 K in the insulating phase,

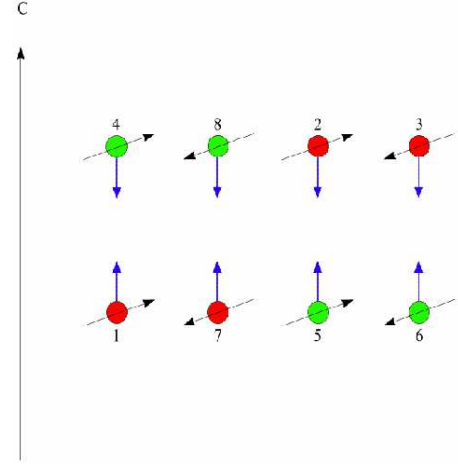


FIG. 3: Antiferroelectric structure of  $(V_{0.972}Cr_{0.028})_2O_3$  at high temperature, as inferred from crystallographic data reported in Ref. [19].

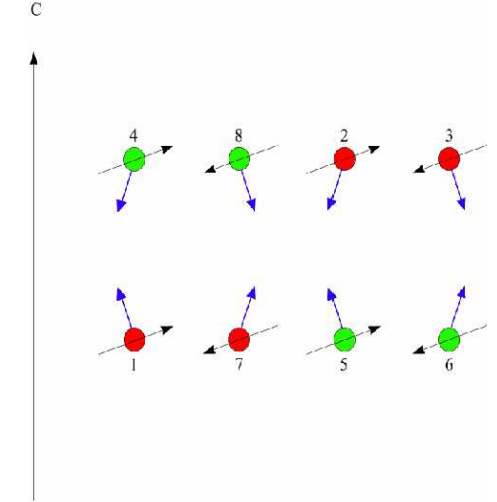


FIG. 4: Tilting of the electric moments in the monoclinic phase of  $(V_{0.972}Cr_{0.028})_2O_3$ . (The arrows at about 71° with respect to the c axis denote the magnetic moments.)

$(V_{1-x}Cr_x)_2O_3$  is an antiferroelectric (AFE) crystal [20].

At  $T = T_N$ , the crystal makes a nearly second-order transition to an AFM monoclinic phase [21]. The driving mechanism of this transition is not fully understood [22]. The lattice space group lowers to  $I2/a$ , with magnetic point group  $C_{2h}$  [23]. Notice that this symmetry is incompatible with the observation of XNLD. However, a reduction of magnetic symmetry leading to  $C_{2h}$  ( $C_{1h}$ ) or  $C_{2h}$  ( $C_2$ ) might take place [24].

A lowering of magnetic symmetry could occur as follows. The structural change to the monoclinic phase eliminates the three-fold axis, which characterises the corundum structure. It probably involves a co-operative

Jahn-Teller distortion, which tilts the electric moments. A tilting with the pattern depicted in Fig. 4 would render  $(V_{1 \times C_{2v}})_2O_3$  an AFM, AFE, and ME crystal, thus explaining the observations of Goulon and his collaborators.

A physical interpretation of Eq. (7) is obtained by expanding the "energy" function  $W(n; L)$  [25]. The  $m$ th term in the MacLaurin formula reads:  $\frac{1}{m!} n_{\alpha} L_{\alpha}^m W(0; 0)$ ; here, greek letters denote cartesian components and repeated indexes are summed over. It is readily seen that  $[L; n]^{(2)}$  stems from the  $m = 2$  term and describes a linear ME effect. The contribution  $[L; L]^2$ ;  $^{(3)}$  is found in the  $m = 4$  term and accounts for a trilinear ME effect.

### 3. XM D

The third form of E1-E2 x-ray dichroism, namely XM D, was probed by Goulon and co-workers [11] at the chromium K-edge in  $Cr_2O_3$  by implementing a new experimental technique: the dichroism of unpolarised x rays. A microscopic description of this spectroscopy, which is readily obtained from our theory of integrated spectra, is reported in the current subsection.

As is known [5], the following integral relationship holds for pure E1 transitions

$$\sum_{j_1+j_2} \frac{(\epsilon_1 + \epsilon_2)_{E1}}{(\sim!)^2} d(\sim!) = 4 \sum_{l=1}^{\infty} \frac{2 n_h(l)}{3 \cdot 2l+1} + b^{(2;+)}(\epsilon; l) h_{lj}^X (3L_z^2 - L^2) \sum_i P_{l-1}^{(1)} \hat{j}_i^2; \quad (10)$$

where  $n_h(l) = 4l+2 h_{lj} \sum_i \hat{j}_i$  denotes the number of holes in the valence  $d$  shell, and  $P_{l-1}^{(1)} = \frac{1}{4} \sum_i \hat{j}_i R_{l-1}^{(1)}$ .

Furthermore,

$$b^{(2;+)}(\epsilon; l) = \frac{1(l+1)[3l(l+1)+1-6l(\epsilon+1)]+3l(\epsilon+1)[l(\epsilon+1)-3]}{6l(2l-1)(2l+1)(l+1)(2l+3)} \quad (11)$$

In the case of a magnetoelectric crystal, E1-E2 corrections to Eq. (10) need to be taken into account. They

read

$$\sum_{j_1+j_2} \frac{(\epsilon_1 + \epsilon_2)_{E1-E2}}{(\sim!)^2} d(\sim!) = \frac{2}{\sim c} \sum_{l=1}^{\infty} (2l+1) R_{l-1}^{(1)} R_{l-1}^{(2)} \frac{2}{5} a_{l^0}^{(1;+)}(\epsilon; l) k_z h_{lj}^X (l; l^0)_z \sum_i \hat{j}_i^2 + \frac{16}{10} a_{l^0}^{(3;+)}(\epsilon; l) k_z h_{lj}^X [L; L]^2; \quad \sum_z (l; l^0)_z \sum_i \hat{j}_i^2 \quad (12)$$

with

$$a_{l^0}^{(1;+)}(\epsilon; l) = \frac{(l+1+l^0)(l+1-2l^0)h_1(l; l; l^0)}{(l+1)(l+1+2)(l+l^0+1)^2}; \quad (13)$$

where  $h_1(l; l; l^0) = l+2l^0-1$  and  $l^0 = l-1$ . We have set  $k = k_z \hat{z}$  in Eqs. (10-12).

Eqs. (10-12) indicate that XM D is observed as follows. Record the  $\epsilon_1 + \epsilon_2$  spectrum in a magnetoelectric

crystal annealed in the parallel configuration. Ditto for antiparallel annealing. Subtract the two spectra.

It goes without saying that such a dichroic spectrum, which is described by Eq. (12), reflects ME properties of crystals.



### III. DISCUSSION AND OUTLOOK

To provide a theoretical interpretation of recent x-ray experiments, which have detected XNCD, XNLD and XM D respectively in  $\text{-LiIO}_3$ ,  $(\text{V}_{0.972}\text{Cr}_{0.028})_2\text{O}_3$  and  $\text{Cr}_2\text{O}_3$ , the current paper has presented a theoretical analysis of near-edge absorption of polarised x rays in noncentrosymmetric crystals. Our work has centred on the derivation of integral relations for dichroic effects which stem from E1-E2 inner-shell excitations. Such relations are written out in terms of one-electron effective operators (order parameters), which identify crystalline microscopic properties revealed by the observed spectra. Two classes of parity-breaking order parameters have been found, which correspond to polar and magnetoelectric moments of valence electrons. Only orbital degrees of freedom have been considered in our derivation; inclusion of spin would be straightforward.

We remind the reader that two irreducible tensors, namely  $O^{(1;+)} = n$  and  $O^{(3;+)} = [L; L]^{(2)}; n]^{(3)}$  (see Section IIA), have not entered our discussion of integrated XNCD, XNLD and XM D spectra. As previously observed,  $O^{(1;+)}$  and  $O^{(3;+)}$  have vanishing geometrical factors and do not appear in our coupled expansion of expression (2). They do contribute however to x-ray resonant dichroism, as can be verified by extending the work of Luo et al. [26] to include E1-E2 processes. (Such a lengthy derivation will not be reported here.) The result is of interest as it indicates the possibility of detecting Bragg peaks from ferroelectric and AFE structures with x rays at resonance.

In conclusion, the pioneering experiments of Goulon and his collaborators appear to have paved the way for new investigations of electronic states in noncentrosymmetric crystals using x-ray absorption and resonant scattering. As shown by our work, a variety of one-electron properties, which result from parity-nonconserving electron interactions, can be measured, yielding valuable information in condensed matter physics and material science.

#### Acknowledgments

Stimulating discussions with F. de Bergevin, P. J. Brown, J. Goulon, and E. Katz are gratefully acknowledged.

We would like to thank S. Dimatteo for pointing out an error in an earlier version of Eq. (7). We are indebted to B. G. Searle for providing the computer program that generated Fig. 1.

\*

### APPENDIX A: SYMMETRY ANALYSIS

Lie groups (or, alternatively, Lie algebras) furnish a powerful tool for interpreting x-ray dichroism in noncentrosymmetric crystals. In fact, effective microscopic operators, which express electronic properties revealed by the spectra, are readily deduced from the pertinent group generators. Our approach hinges therefore on spectrum-generating algebras, a concept originally introduced in nuclear [27] and particle physics [28, 29].

We follow Carrara and Benoist [30] and consider the general framework of a de Sitter algebra:  $so(3;2)$  [27, 31]. A realisation of such an algebra is provided by the operators:

$$A = i(A - A^\dagger) = 2; \quad A^\dagger = (A + A^\dagger) = 2; \quad (\text{A } 1)$$

$$L \quad \text{and} \quad N_0; \quad (\text{A } 2)$$

where  $L$  denotes the orbital angular momentum (in units of  $\hbar$ ) and  $N_0 |j m\rangle = (l + \frac{1}{2}) |j m\rangle$ , with  $|j m\rangle$  a spherical harmonic. Furthermore,

$$A = n f_1(N_0) + r f_2(N_0); \quad (\text{A } 3)$$

with  $n = r = r$ ,  $r = i$  in  $L$  and

$$f_1(N_0) = (N_0 - 1/2) f_2(N_0); \quad (\text{A } 4)$$

$$f_2(N_0) = \frac{P}{(N_0 - 1)N_0}; \quad (\text{A } 5)$$

$A$  and  $A^\dagger$  are known as shift operators as their action on  $|j m\rangle$  changes  $l$  into  $l \pm 1$ .

A physical interpretation of  $A$  is provided by the relation

$$= (n \quad L \quad L \quad n) = 2 = i n; L^2 = 2 = \frac{i}{2} r \quad r^\dagger = \frac{1}{2} \frac{1}{N_0} N_0; A + \frac{1}{N_0}; \quad (\text{A } 6)$$

where  $[[:::]]_+$  denotes an anticommutator. Eq. (A 6) denotes the (purely angular) orbital anapole [32, 33, 34].

A physical representation of the generator  $A^\dagger$  is provided by

$$A^\dagger = \frac{P}{N_0 n} \frac{P}{N_0}; \quad (\text{A } 7)$$

$L_z$  and  $L_{\pm}$  provide the building blocks of our derivation. They form a triad of mutually orthogonal dimensionless vectors. Their nature (magnetic, electric and magnetoelectric, respectively) is readily inferred from behaviour under space inversion and time reversal.

Notice that  $L$  (rotations) and  $N$  (boosts) generate a homogeneous Lorentz group:  $SO(3,1)$ . Also  $L$  and  $N_0$  and  $N_{\pm}$ , where  $N_0 |j m\rangle = (1 + \frac{1}{2}) |j m\rangle$ , generate

$SO(3,1)$ . The homogeneous Lorentz group enters our derivation of I-odd operators in a natural way, given its deep interweaving with chirality. Notice that  $L$ ,  $N_0$  and  $N_{\pm}$  provide a realisation of the  $so(3;2)$  de Sitter algebra. This is the required symmetry extension, with respect to pure E1 or E2 transitions, that was mentioned in the Introduction.

- 
- [1] D. H. Templeton and L. K. Templeton, *Acta Crystallogr. A* 36, 237 (1980).
- [2] G. Schutz, W. Wagner, W. Wilhelm, P. Kienle, R. Zeller, R. Frahm, and G. Materlik, *Phys. Rev. Lett.* 58, 737 (1987).
- [3] B. T. Thole, P. Carra, F. Sette, and G. van der Laan, *Phys. Rev. Lett.* 68, 1943 (1992).
- [4] P. Carra, B. T. Thole, M. Altarelli, and X. D. Wang, *Phys. Rev. Lett.* 70, 694 (1993).
- [5] P. Carra, H. Konig, B. T. Thole, and M. Altarelli, *Physica B* 192, 182 (1993).
- [6] R. Benoist, P. Carra, and O. K. Andersen, *Eur. Phys. J. B* 18, 193 (2000).
- [7] X-ray dichroism implies excitations from inner shells, which are filled in the ground state and can therefore be 'integrated out'. As a result, one-electron properties of valence states are probed in the x-ray region.
- [8] L. Alagna, T. Prospero, S. Turchini, J. Goulon, A. Rogalev, C. Goulon-Ginet, C. R. Natoli, R. D. Peacock, and B. Stewart, *Phys. Rev. Lett.* 80, 4799 (1998).
- [9] Goulon J., C. Goulon-Ginet, A. Rogalev, V. Gotte, C. Malgrange, C. Brouder, and C. R. Natoli, *J. Chem. Phys.* 108, 6394 (1998).
- [10] J. Goulon, A. Rogalev, C. Goulon-Ginet, G. Benayoun, L. Paolasini, C. Brouder, C. Malgrange, and P. A. Metcalfe, *Phys. Rev. Lett.*, 85, 4385 (2000).
- [11] J. Goulon, A. Rogalev, F. Wilhelm, C. Goulon-Ginet, P. Carra, D. Cabaret, and C. Brouder, *Phys. Rev. Lett.* 88, 237401 (2002).
- [12] I. E. Dzyaloshinskii, *J. Exptl. Theoret. Phys. (U. S. S. R.)* 37, 881 (1959) [translation: *Soviet Phys. JETP* 10, 628 (1960)].
- [13] D. A. Varshalovich, A. N. Moskalev, and V. K. Khersonskii, *Quantum Theory of Angular Momentum* (World Scientific Publishing, Singapore, 1988).
- [14] Integration is over a finite energy interval, which corresponds to the two partners of a spin-orbit split inner shell.
- [15] Sum rules for pure E1 or E2 transitions were derived by representing valence-electron states within an  $|j m\rangle$  basis. In this case, the pertinent order parameters are derived from the generators of rotation groups: the components of spin and orbital angular momentum. Such a formulation can be extended to include parity-conserving hybridisation; for example, it can be shown that pure E1 linear dichroism mixes  $|j m\rangle$  and  $|j-1, 2m\rangle$ . Discussion of these effects is beyond the scope of the current paper.
- [16] In Eq. (5), the radial integrals are defined by
- $$R_{l_1 l_2}^{(L)} = \int_0^Z dr' r'_{l_1}(r) r'^{L+2} r'_{l_2}(r);$$
- where  $r'_{l_1}(r)$  and  $r'_{l_2}(r)$  denote inner-shell and valence radial wave functions, respectively. Our derivation neglects relativistic corrections to the radial part of the atomic wave functions.
- [17] It is the magnetic field of the so-called magnetoelectric annealing, a standard technique for creating a single magnetoelectric domain in the crystal.
- [18] P. D. Demier and M. Marezio, *Phys. Rev. B* 2, 3771 (1970).
- [19] P. D. Demier, *J. Phys. Chem. Solids* 31, 2569 (1970).
- [20] Notice that  $x = 0.038$  in Ref. 20 and  $x = 0.028$  in Ref. 10. As shown by the phase diagram of M cWhan and Remeika [*Phys. Rev. B* 2, 3734 (1970)], the two substitutions are equivalent.
- [21] R. M. Moon, *Phys. Rev. Lett.* 25, 527 (1970).
- [22] M. Yethiraj, S. A. Werner, W. B. Yelon, and J. M. Honig, *Phys. Rev. B* 36, 8675 (1987).
- [23] S. Di Matteo, N. B. Perkins, and C. R. Natoli, *Phys. Rev. B* 65 054413 (2002).
- [24] These two ME point groups are subgroups of  $C_{2h}$   $R$ ; in international notation they are denoted by  $2/m$  and  $2/m$ , respectively.
- [25] The method is expounded in L. D. Barron, *Molecular Light Scattering and Optical Activity* (Cambridge University Press, Cambridge, 1982); Chapter 2.
- [26] J. Luo, G. T. Trammell, and J. P. Hannon, *Phys. Rev. Lett.* 71, 287 (1993).
- [27] S. Goshen and H. J. Lipkin, *Ann. Phys. (N. Y.)* 6, 301 (1959); and in *Spectroscopic and Group Theoretical Methods in Physics - Racah Memorial Volume*, F. Bloch et al. Eds., North-Holland, Amsterdam, 1968.
- [28] Y. Dathan, M. Gellmann, and Y. Ne'eman, *Phys. Lett.* 17, 148 (1965); N. Mukunda, L. O'Riadaigh and E. C. G. Sudarshan, *Phys. Rev. Lett.* 15, 1041 (1965).
- [29] Y. Dathan and Y. Ne'eman, *Band Spectra Generated by Non-Compact Algebras*, reprinted in F. J. Dyson, *Symmetry Groups in Nuclear and Particle Physics - A Lecture Note and Reprint Volume*, Benjamin, New York, 1966.
- [30] P. Carra and R. Benoist, *Phys. Rev. B* 62, R7703 (2000).
- [31] M. J. Engle, *Group Theory and the Coulomb Problem*, Wiley-Interscience, New York, 1972.
- [32] Ya. B. Zeldovich, *Zh. Eksp. Teor. Fiz.* 33, 1531 (1957) [*Sov. Phys. JETP* 6, 1184 (1958)].
- [33] V. V. Flambaum and I. B. Khriplovich, *Zh. Eksp. Teor. Fiz.* 79, 1656 (1980) [*Sov. Phys. JETP* 52, 835 (1980)].
- [34] M. A. Bouchiat and C. Bouchiat, *Rep. Prog. Phys.* 60,